Electrical Interface Barriers*

T.C. McGill and C.A. Mead

Abstract—A review of the phenomena associated with electrical barriers between metals, and insulators and semiconductors is presented. The observed phenomenological rules governing the value of the barrier energies for different metals on the same insulator or semiconductor are presented. The barrier energies on ionic insulators are shown to vary strongly with the metal. While in the case of covalent semiconductors, the barrier energies are relatively independent of the metal. The barrier energy from the metal to the conduction band of the semiconductor is shown to be approximately two-thirds of the semiconductor band gap with certain exceptions. Transport through interfacial barriers is illustrated by discussing the transport through metal–GaSe–metal structures and Mg–SiO_2 structures. Both thermal-induced transport over the barrier, and tunneling through the barriers are discussed.

1 Introduction

The study of electrical interface barriers dates back to 1874, when K. F. Braun [1] observed that an interface formed by a metal wire brought into contact with a lead sulfide crystal carried current more easily in one direction than in the other. While this result was rather puzzling at the time, it can be explained by postulating that a certain energy is required to take an electron from the Fermi energy of the metal and place it in the conduction band of the lead sulfide crystal. This energy is called the interfacial barrier energy ϕ_B. Since that first observation, interfacial barriers have been studied extensively by a large number of workers [2]. In this paper, we would like to summarize some of the results of these investigations.

We divide our discussion into two parts. First, we summarize a series of empirical rules which tell how the magnitude of the barrier energy varies as we change the metal on a given insulator or semiconductor, and how large the barrier energies are on a covalent semiconductor. Second, we discuss the various modes of current transport across (or through) interfacial barriers.

2 Empirical Rules for Barrier Energies

From the study of the size of ϕ_B for a rather large number of semiconductors and insulators, two empirical rules have been noted. The first of these rules deals with the variation of ϕ_B on a given insulator or semiconductor as we change the metal. The second deals with the magnitude of ϕ_B for metals on covalent semiconductors.

*Re-typeset from original material by Donna Fox, July 2017. Originally published in *J. Vac. Sci. Technol.,* Vol. 11, No. 1, Jan./Feb., 1974. This paper was supported in part by AFOSR under Grant No. 73-2490, and in part by ONR under Grant No. N00014-67-A-0094-0017.

Let us start with the first of these two rules. Simple considerations of how the barrier forms [3] suggests ϕ_B should be written as the difference of two quantities: one characteristic of the metal vacuum interface, and the other characteristic of the insulator or semiconductor-vacuum interface. The first of these is the work function of the metal ϕ_W, the energy required to take an electron from the Fermi energy of the metal into the vacuum; and the second is the electron affinity of the insulator of semiconductor x_s, the energy gained by taking an electron in vacuum and placing it at the bottom of the conduction band of the semiconductor or insulator. That is,

$$\phi_B = \phi_W - x_s. \tag{1}$$

Accurate values of ${\phi_W}^4$ are not readily accessible for all the metals of interest; hence, we will use instead the electronegativity [5] of the metal X_M, a quantity which is readily available. The values of ϕ_W are closely related to those of X_M except for a constant. This substitution has no important effect on the results that are to follow. Hence, we have that

$$\phi_B = X_M - x_s + \text{const}, \tag{2}$$

where X_M is the electronegativity of the metal. This simple argument would lead us to conclude that the barrier energy should increase linearly as we vary the electronegativity of the metal with a slope of unity. More generally, we might write that

$$\phi_B \cong SX_M + \text{const}, \tag{3}$$

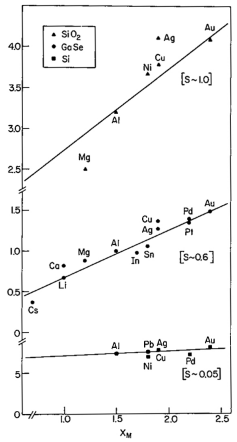

Figure 1: Barrier energies of various metals on SiO_2, GaSe, and Si plotted vs. the electronegativity X_M of the metal. S is the slope of the line drawn through the experimental points.

where S is the slope of the variation of the barrier energy with the electronegativity of the metal. The simple theory would suggest that S should be unity.

In Fig. 1, we have plotted the values of ϕ_B vs. X_M for three different insulators or semiconductors—SiO_2, GaSe, and Si. In the case of SiO_2, the slope S is approximately one. While in the case of GaSe, it is 0.6; and in the case of Si, it is approximately zero. This shows that the values of S can be quite different from the simple theory; and, since SiO_2 is more ionic than GaSe, which in turn is more ionic than Si, it suggests that the value of S depends upon the ionicity of the semiconductor or insulator. To illustrate this point further, we take as a measure of the ionicity of an AB compound [5], [6] the difference in the electronegativities of the two constituents

$$\Delta X = X_B - X_A, \tag{4}$$

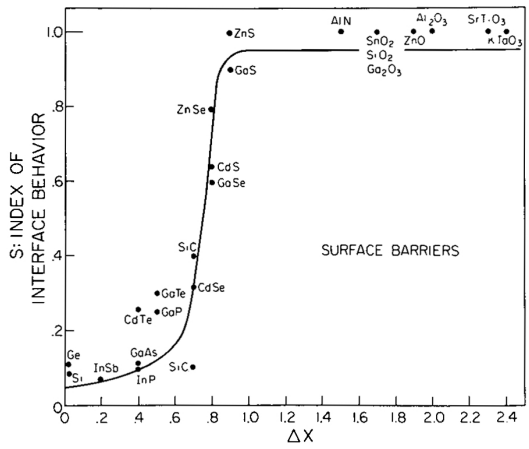

Figure 2: The slope of the line through the barrier energies as a function of the electronegativity X_M of the metal as a function of the electronegativity difference of the insulator or semiconductor.

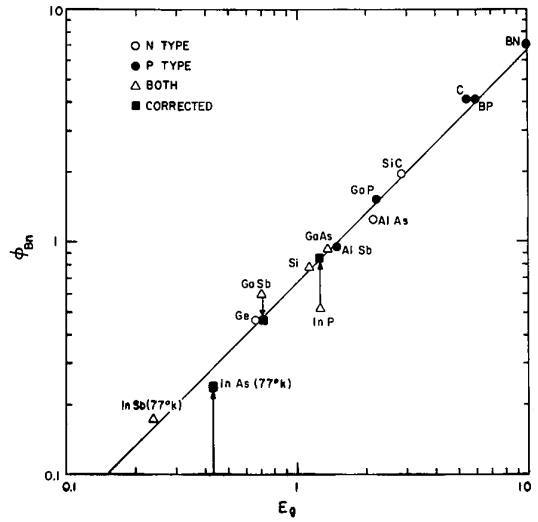

Figure 3: Barrier energies for zinc-blende materials as a function of the band gap of the semiconductor. See [14] for the method of obtaining the corrected values.

where X_A is the electronegativity of the species A, and X_B is the electronegativity of the species B. Then, if we plot S vs. ΔX, we obtain the rather surprising results shown in Fig. 2 [7]. The value of S is quantitatively determined by ΔX with S remaining small for $\Delta X < 0.7$ and then changing rather rapidly to a value of S equal to unity for $\Delta X > 0.7$. That is, for ionic materials where $\Delta X > 0.7$, ϕ_B varies directly with the electronegativity of the metal. While for $\Delta X < 0.7$, ϕ_B depends rather weakly on the electronegativity of the metal.

Since the behavior of the more ionic materials can be understood qualitatively in terms of the simple ideas mentioned above, most theoretical effort [8]–[13] has been concentrated upon accounting for the behavior of the more covalent materials and explaining why an abrupt transition in behavior should occur when $\Delta X \approx 0.7$.

The second empirical rule for barriers deals with the magnitude of the barrier energy of a metal on covalent semiconductors. If one studies the size of ϕ_B for the covalent semiconductors one finds, with a few exceptions, that the barrier energy is at approximately $\frac{2}{3}$ the band gap E_g [14]. To illustrate this point, we have plotted the barrier energy of Au on a number of different covalent semiconductors as a function of

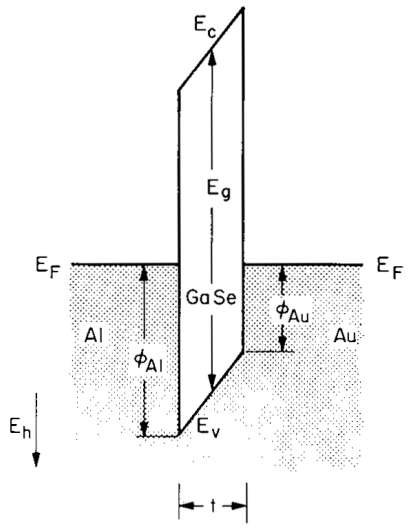

Figure 4: Energy band diagram of an Al–GaSe–Au structure under zero-applied bias. Hole energy increases down E_g in the bandgap of GaSe, 2.0 eV. ϕ_{Al} is the Al–GaSe barrier energy, 1.05 eV. ϕ_{Au} is the Au–GaSe barrier energy, 0.52 eV. E_F is the Fermi level.

the band gap of the semiconductor in Fig. 3. The straight line in the figure is the line $\phi_B = 2E_g/3$.

In summary, the barrier energy varies according to Eq. 2 for metals on ionic materials and is relatively independent of the metal for metals on covalent semiconductors. For metals on covalent semiconductors, the barrier energy is approximately $\frac{2}{3}$ of the band gap.

3 Electrical Transport Over and Through Interfacial Barriers

The electrical barrier at the interface between a metal and an insulator or semiconductor can be explored experimentally by studying the transport of current through the interface. This can be accomplished in two ways: first, by exciting electrons over the barrier using light and studying the photocurrent [2]; and second, by measuring the current transport due to electrons which are thermally excited over the barrier [15] or owing to electrons which tunnel through the barrier [16]. In this paper, we concentrate upon the second of these two methods.

One of the simplest ways of studying the influence of the interfacial barrier on current transport is to make samples in which the insulator is sufficiently thin that current transport is limited by the interfacial barrier. Such a structure consisting of Al, a thin layer of GaSe, and Au is shown in Fig. 4. In this case, the barrier energies are measured from the Fermi level of the metal to the valence band of the GaSe. The values of the various parameters relevant to GaSe are given in [15].

If the thickness of the GaSe layer is greater than a few-hundred angstroms, then the current is carried by carriers which are thermally excited over the barrier. Hence, the current should vary as the number of carriers which have a thermal energy large enough to surmount the barrier. That is,

$$J \simeq J_0 \exp\left(-\phi_{\mathrm{eff}}/k_B T\right), \tag{5}$$

where ϕ_{eff} is the barrier height limiting the current flow. Current-voltage characteristics, $I - V$, like those given by Eq. 5 are observed in Au–GaSe–Al structures as shown in Fig. 5. In the "low forward," the

current flow of holes from the Au is limited by the Al–GaSe barrier which is reduced in value with respect to the Fermi level of Au. In the "high forward," the current flow of holes from the Au is limited by the Au–GaSe barrier, which in the first approximation does not move with respect to the Fermi level of the Au. However, once the image of the carrier in the insulator in the metal is included in the calculation of the barrier shape, the barrier becomes field-dependent and lowers slightly with increasing bias [15]. This leads to the observed increase of current with voltage.

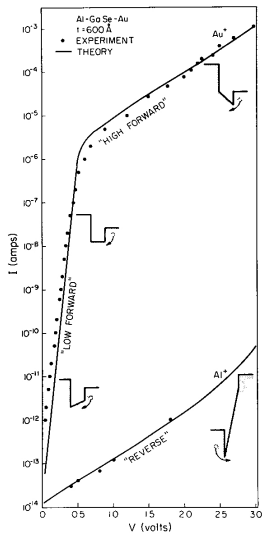

Figure 5: Current–voltage characteristic of an Al–GaSe–Au structure. The dots are experimental data; the solid line is calculated as described in [15]. The insets show the partial band diagram of the Al–GaSe–Au structure, and illustrate the various bias conditions.

In the "reverse direction," the current is due to holes from the Al and is limited by the Al–GaSe barrier. As in the case of the "high forward," the barrier height should vary slowly with bias due to the image lowering of the barrier. However, the current increases more sharply than predicted by the simple image lowering. The rather large rate of increase of the current with applied bias is due to the fact that the barrier can become so sharply peaked at high biases that holes can actually tunnel through the top of the barrier. This phenomenon is illustrated in Fig. 6, where we have plotted the distribution of current due to holes as a function of hole energy along the barrier shape. As can be seen from this figure, the current at small biases is carried mainly by carriers coming over the top of the barrier. While at large biases, the current is due mainly to the electrons which have been thermally excited and then tunnel through the top of the barrier.

One simple experimental verification of the current expression given in Eq. 5 is the temperature dependence of the current. One would expect that the current for fixed voltage should decrease exponentially with $1/T$ with a slope given by the barrier energy divided by Boltzmann's constant. In Fig. 7, we have the results of measuring the temperature dependence of the current when the sample is biased in the "high forward." The correct exponential activation of the current is observed.

For very thin samples less than 100-$\mathring{A}$ thick, the current-voltage characteristic of the devices are different from those observed for devices with thicker insulators. In this case, the current is due to the tunneling of electrons through the insulator. One might expect that the wave-function of the tunneling electron would be exponentially attenuated as it passes through the insulator. The attenuation would in the simplest case (of relatively small electric field) be dependent upon the energy of the electron relative to the valence band. Hence, we would expect that the probability of an electron in the metal with a given energy E

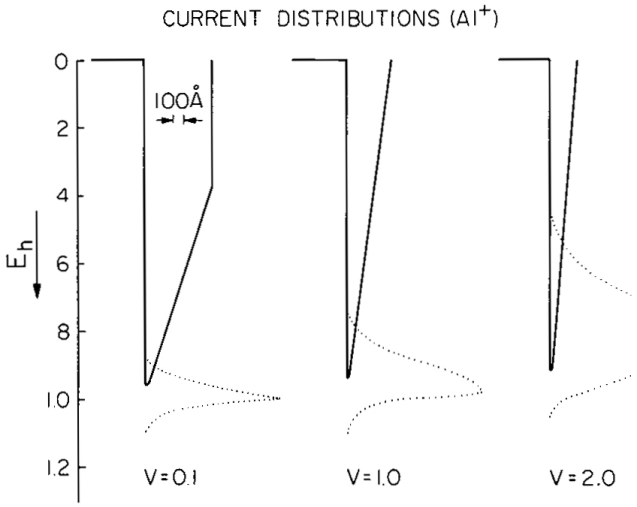

Figure 6: Theoretical (normalized) current distribution for a reverse-biased 600-Å-thick Al–GaSe–Au structure. The solid curves illustrate the shape of the image-lowered potential barrier; the dotted curves represent the distribution, as a function of hole energy E, of the injected carriers.

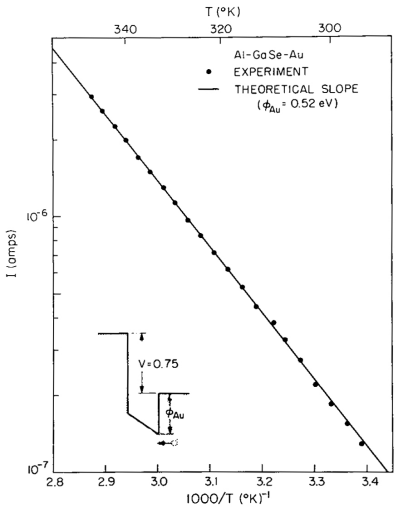

Figure 7: Current as a function of $1000/T$ for the Au electrode buried +0.75 V on a 600-Å-thick Al–GaSe–Au structure. The dots are experimental data; the solid line is calculated as described in [15].

tunneling would be given by

$$P(E) = \exp\left[-2\int k\left(\epsilon\right) dx\right], \tag{6}$$

where $k(\epsilon)$ is the decay constant for a given energy ϵ measured with respect to the valence band or conduction band of the insulator and the integral is taken over the distance x, in which the electron is in the forbidden gap of the insulator. We can distinguish two cases: one in which the electron has an energy such that it is in the forbidden gap of the insulator during the entire distance across the insulator, and one in which the electron has an energy such that it is in the forbidden gap of the insulator only during part of the distance across the insulator. We discuss the former case first.

In this case, the total current-density J would be given by the integral over those electrons which are

below the Fermi energy of one metal, and above the Fermi energy of the other metal [16]. That is

$$J = A \int dE\ P(E), \tag{7}$$

where A is approximately constant [16]. In the case of GaSe, all the tunneling characteristics can be explained by using the function $k(\epsilon)$ given in Fig. 8. (The zero of energy is taken at the valence band edge in this figure.)

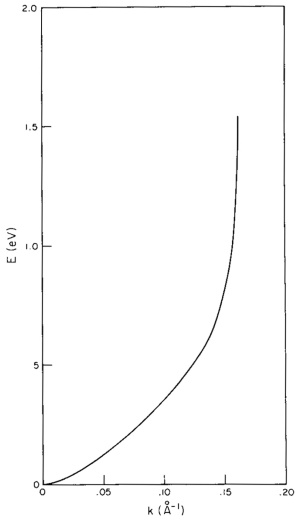

Figure 8: The attenuation constant of the electronic wave-function vs. energy for GaSe. The way in which the function was obtained is described in [16].

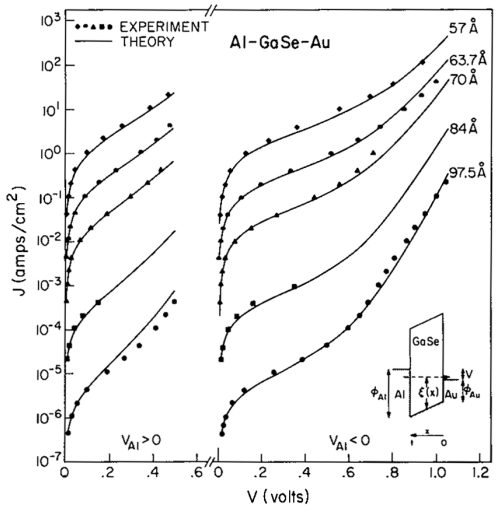

Figure 9: Current-voltage curves, for both directions of applied bias, of a number of Al–GaSe–Au structures. Solid symbols represent experimental data. The solid lines are theoretical curves obtained in a manner described in [16].

Typical experimental current voltage, $I - V$, characteristics as a function of thickness are shown in Fig. 9. In this figure, we have also included the current voltage characteristic to be expected from an equation

similar to Eq. 7 [16]. The agreement of the experimental $I-V$ with the theoretical $I-V$ for a number of different thicknesses using a single function $k(\epsilon)$ verifies at least qualitatively that the tunneling model gives a good account of the $I-V$ characteristics. To give some idea of how the distribution of tunneling electrons change as we vary the thickness of the insulator, we have plotted the current distribution for a few voltages in Fig. 10. From this figure, one can see the big difference in the current distributions for the two different thicknesses. Finally, we might consider the result of changing one of the interfaces. That is, we replace the Al by Cu and measure the $I-V$ characteristic of an Au–GaSe–Cu structure. The resulting $I-V$ characteristic is shown in Fig. 11 along with the theoretical $I-V$ computed from Eq. 7. The agreement is quite good.

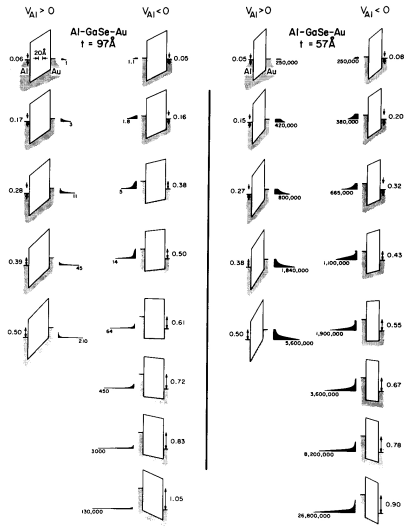

Figure 10: Energy distributions of tunneling electrons and corresponding band diagrams for two Al–GaSe–Au structures. The calculation of these distributions is described in [16]. The number beneath the peak of each distribution indicates the absolute magnitude of the peak relative to the peak of every other distribution in the figure.

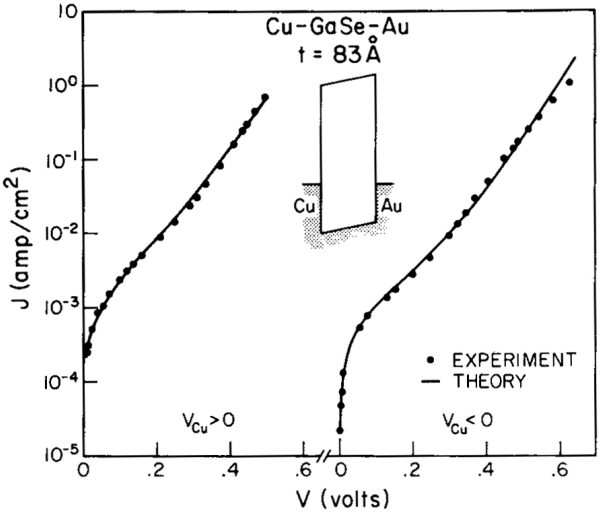

Figure 11: Experimental current-voltage curve of an 83-Å-thick Cu–GaSe–Au structure is shown by the solid symbols. The solid curve is the theoretical current-voltage curve described in [16].

Finally, we take up the second type of tunneling called Fowler Nordheim tunneling [17]. In this mechanism of current flow, an electron nears the Fermi energy of the metal tunnels into the insulator, and then is

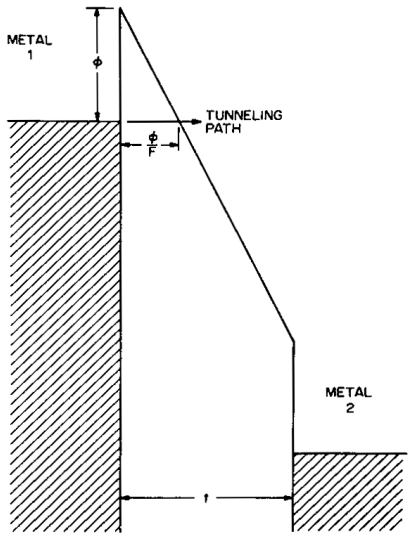

Figure 12: Energy diagram of a thick metal insulator-metal structure under high-applied bias. Note that the tunneling distance is ϕ/F.

transported across the insulator into a second collecting metal (see Fig. 12). In this situation, the current is given by the probability that the electron tunnels through the uppermost triangular part of the barrier. The distance that the electron has to tunnel is given by ϕ/F where F is the applied field (see Fig. 12). Hence, the current voltage characteristic should go as

$$J = J_0 \exp\left[\frac{-2\phi\overline{k}}{F}\right], \tag{8}$$

where $\overline{k}$ is the average decay constant of the wave-function in the insulator at energies from ϕ to the conduction band. Experimental $I - V$ characteristics for Mg–SiO_2 interface [18] is given in Fig. 13 where the log of J is plotted as a function of the reciprocal of the field. The agreement is quite good between theory and experiment.

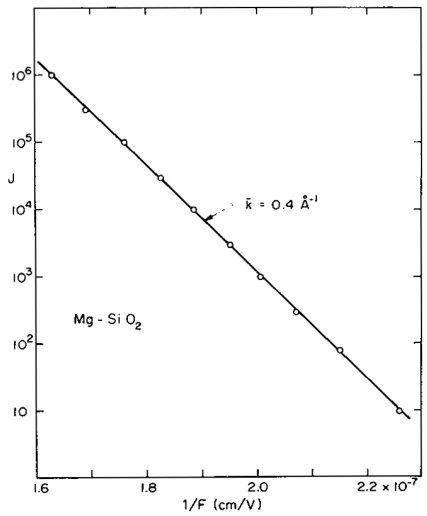

Figure 13: Fowler Nordheim plot of the current-voltage characteristics of SiO_2–Mg (after [18]). The current is normalized such that it is one at the lowest fields.

4 Summary

In summary, we have reviewed some of the empirical rules governing the barrier energies at metal semiconductor and metal insulator contacts, and found that there are some striking regularities in the variation and magnitude of the barrier energies. We have also reviewed the various modes of current transport through interfaces and shown that there is quite good qualitative, if not quantitative, agreement of the experimental results with highly-simplified model theories of transport through interfaces.

References

[1] K. F. Braun, Ann. Phys. Pogg. **153**, 556 (1874).

[2] C. A. Mead, Solid State Electronics **9**, 1023 (1966).

[3] A. Many, Y. Goldstein, and N. B. Grover, Semiconductor Surfaces (North-Holland, Amsterdam), p. 131 (1965).

[4] J. C. Riviere, "Work Function: Measurements and Results," unpublished report of the Metallurgy Division of Atomic Energy Research Establishment at Harwell, U.K. (1967).

[5] L. Pauling, The Nature of the Chemical Bond, 3rd ed. (Cornell U. P., Ithaca, New York), p. 93 (1960).

[6] J. C. Phillips, Rev. Mod. Phys. **42**, 317 (1970).

[7] S. Kurtin, T. C. McGill, and C. A. Mead, Phys. Rev. Lett. **22**, 1433 (1969).

[8] J. Bardeen, Phys. Rev. **71**, 717 (1947).

[9] V. Heine, Phys. Rev. A **138**, 1689 (1965).

[10] J. C. Phillips, Solid State Commun. **12**, 861 (1973).

[11] J. C. Inkson, J. Phys. C **6**, 1350 (1973).

[12] B. Pellegrini, Phys. Rev. B **7**, 5299 (1973).

[13] E. Louis and F. Yndurain, Phys. Status Solidi **57b**, 175 (1973).

[14] C. A. Mead and W. G. Spitzer, Phys. Rev. **134**, A713 (1964).

[15] T. C. McGill, S. Kurtin, L. Fishbone, and C. A. Mead, J. Appl. Phys. **41**, 3831 (1970).

[16] S. L. Kurtin, T. C. McGill, and C. A. Mead, Phys. Rev. B **3**, 3368 (1971).

[17] R. H. Fowler and L. W. Nordheim, Proc. Roy. Soc. (London) **A119**, 173 (1928).

[18] M. Lenzlinger and E. H. Snow, J. Appl. Phys. **40**, 278 (1969).